Journal of Materials Chemistry C

PAPER

Cite this: J. Mater. Chem. C, 2015, 3, 12316

Flexible inorganic–organic thin film phosphors by ALD/MLD

Z. Giedraityte, P. Sundberg and M. Karppinen*

Received 6th October 2015,
Accepted 8th November 2015

DOI: 10.1039/c5tc03201f

www.rsc.org/MaterialsC

Inorganic–organic europium-based hybrid materials have good luminescent properties and play a key role in many important optical applications, such as nanosized phosphorescent and optoelectronic devices. Here we demonstrate the feasibility and potential benefits of synthesizing such materials with a direct deposition method with atomic/molecular level precision using the emerging atomic layer deposition/molecular layer deposition (ALD/MLD) technique. Such a process allows for fundamentally new types of highly uniform and conformal hybrid inorganic–organic thin films by alternating exposures of inorganic and organic reactants on flexible/sensitive/nanostructured surfaces. We employ $Eu(thd)_3$ and 3,5-pyridinedicarboxylic acid as precursors and deposit the films on a variety of substrate materials in the temperature range from 240 to 400 °C. The appreciably fast self-limiting surface reactions yield thin films with high luminescence intensities. We foresee that our Eu-hybrid thin-film phosphors grown by ALD/MLD could be exciting new phosphor materials in applications where ultrathin luminescent coatings on flexible and/or nanostructured surfaces are needed.

1. Introduction

Motivation for the synthesis of various Eu-based inorganic–organic complexes stems from their good photoluminescence properties in the visible range relevant to various optical applications.[1–3] Luminescent europium complexes act as light conversion molecular devices, and offer an attractive substituent for the commonly used organic fluorophores due to their photochemical stability, long luminescence lifetimes and sharp emission peaks.[4] The Laporte-forbidden transitions of europium causing weak excitation of electrons are overcome by using a sensitizing chromophore or antenna as a ligand in the complex.[4] Various N-heterocyclic ligands including pyridine, phenanthroline, benzimidazole, pyrazole, oxazoline, hydroxylquinoline, azaxanthone, *etc.*, have been employed as efficient sensitizing chromophores for the photoluminescence of europium; in particular, aromatic pyridine ligands are good candidates for enhancing the luminescence properties of Eu and other lanthanides due to their strong binding abilities to the lanthanide ions.[5,6] The pyridine chromophores incorporated in chelate ligands such as beta-diketonates or carboxylate ligands are known to afford highly stable complexes which prevent the non-radiative decay.[7]

Various synthetic methods have already been successfully employed for the synthesis of such lanthanide based inorganic–organic complexes.[7–9] There are however still a number of challenges to be addressed regarding the synthesis of these luminescent materials set by the specific applications, such as luminescence quenching effects; the need to eliminate OH NH oscillators, enhance the energy transfer and decrease the non-radiative decay.[10] New materials are required possessing enhanced properties. For many cutting-edge applications, such as organic light emitting diodes and solar concentrators, it would be desirable to synthesize the materials as flexible (ultra)thin films, with a precisely controlled thickness over a variety of surface (nano)structures and device architectures.[11,12]

Atomic layer deposition (ALD) is the state-of-the-art industrially-feasible thin-film deposition technique for inorganics, based on successive self-limiting gas-surface reactions of alternating doses of gaseous precursors. Thin films made by ALD are deposited under relatively mild conditions and they exhibit a well-defined composition, density, thickness and uniformity; they are also highly conformal, following various complicated 3D surface nanostructures down to (sub)nanometer precision.[13–15] Recently the technique was extended to organic materials, *i.e.* MLD (molecular layer deposition). Most interestingly to the present work, by combining ALD cycles with MLD cycles it is possible to deposit inorganic–organic hybrid materials in an atomic/molecular layer-by-layer manner.[16–22] Like ALD, the MLD technique is based on sequential and self-limiting gas–solid surface reactions. Despite the huge potential of the ALD/MLD technique for frontier hybrid material synthesis, only a small number of processes have so far been developed where the metal constituents are mostly limited to Al, Zn and Ti; for a recent review, see ref. 22.

Department of Chemistry, Aalto University, FI-00076 Espoo, Finland.
E-mail: maarit.karppinen@aalto.fi

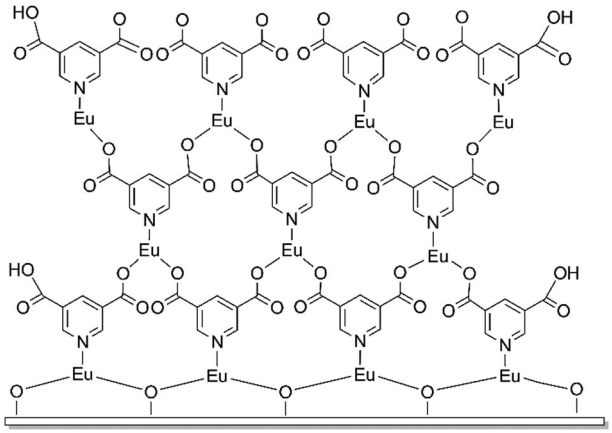

Fig. 1 Illustration of a possible structure of our ALD/MLD-grown Eu-hybrid thin films.

Here we demonstrate the layer-by-layer ALD/MLD growth of novel hybrid Eu-based inorganic–organic thin films with excellent luminescence properties fabricated from $Eu(thd)_3$ (thd: 2,2,6,6-tetramethyl-3,5-heptanedione) and 3,5-pyridine-dicarboxylic acid precursors. The underlining surface reactions are shown to be self-limiting, thus providing a means to deposit highly uniform and conformal coatings with precise control over thickness on various substrates. A schematic illustration of the ideal bonding structure of these films is given in Fig. 1.

2. Experimental section

The ALD/MLD thin-film depositions were performed in a commercial ALD reactor (F-120 by ASM Microchemistry Ltd). The inorganic precursor $Eu(thd)_3$ was prepared in-house,[23] while the organic precursor, 3,5-pyridinedicarboxylic acid, was a commercial product (TCI Europe N.V.). During the depositions, both the $Eu(thd)_3$ and the pyridinedicarboxylic acid precursors were kept in glass crucibles inside the reactor, at 140 and 200–235 °C, respectively. Due to the high volatility of the organic precursor, the latter crucible was covered with quartz glass wool (Nabertherm). Nitrogen (>99.999%; Schmidilin UHPN 3000 N_2 generator) was used as a carrier and purging gas, and a pressure of 2 to 4 mbar was maintained in the reactor during the film deposition.

The film thickness values were determined by X-ray reflectivity measurements (XRR; PANalytical X'Pert MPD Pro Alfa 1). Grazing incident X-ray diffraction measurements with the same instrument were carried out to investigate the crystallinity of the samples. Fourier transform infrared spectroscopy (FTIR; Nicole Magna 750) was used to identify the organic components in the samples. The measurement chamber was purged with dry air, and the spectrum measured for the substrate was subtracted from those for the thin-film samples. The surface chemistry of the films was investigated by using X-ray photoelectron spectroscopy (XPS; AXIS Ultra by Kratos Analytical) with monochromated Al-Kα irradiation at 100 W and the charge neutralizer on. Finally the films were characterized by UV-Visible absorption spectroscopy (Perkin Elmer Lambda 950 UV/Vis/NIR absorption spectrophotometer) and photo-luminescence spectroscopy. The excitation and emission spectra were collected by Quanta Master 40 spectrofluoro-meter from Photon Technology International; in these measurements second order peaks were eliminated by using a 40 nm long pass filter (FGL400, Thorlabs) in the emission channel; the emission and excitation slits used in the measurements were set to 3 nm and the fluorescence spectra were corrected by using instrument's excitation and emission corrections provided by the manufacturer.

Preliminary tests were carried out to evaluate the mechanical properties of the films for their potential use in flexible devices. For the uniaxial stress analysis, the films were deposited on polyimide substrates and then cut into strips of 3 mm wide and 2 cm long by pressing with in-house made razor blade jig. The strips were glued from both ends onto small pads of abrasive paper, allowing a 10 mm long strip available for standard tensile tests. The thickness of the films was measured with a film thickness measurement setup composed of the displacement sensor (26F-011OL-B; Mitutoyo), digital reader (EH-IOP; Mitutoyo), and a measuring table support for sensor (215-514 comparator stand; Mitutoyo). For the mechanical characteri zation the samples were clamped to the tensile tester (Tensile/Compression Module 5 kN with 100 N load cell; Kammrath&Weiss GmbH) at 22 °C and 49% humidity. Rate of the elongation was equal to 0.85 mm min^{-1}, and the gauge length was 10 mm. For the stress analysis the images were taken under an optical microscope (Leica DM 4500P; 10× magnification) and an optical video was recorded with a mounted camera (Canon EOS 60D).

For the dynamic cycling elongation the films were repeatedly stretched 30 times up to 3% elongation and afterwards the film was imaged under an optical microscope. For the bending test, the films deposited on polyimide substrates were cut into 37 mm long and 5 mm wide pieces and further were bended repeatedly 600 times using an in-house made bending test apparatus. The test piece bending radius was decreased by controlling the moving distance to a designated bending radius. The existence of cracks in the surface was monitored by an optical microscope.

3. Results and discussion

In our preliminary deposition experiments we first searched for the optimal precursor/purge pulse lengths; the surface reactions were found to be appreciably fast, resulting in the same growth-per-cycle (GPC) value (within experimental error limits) at a given deposition temperature independent of the pulse lengths of the precursors – a fact that is generally taken as a proof of the saturated self-limiting nature of the reactions; we showed this at the deposition temperature of 290 °C for the pulse length ranges of 1–5 s for $Eu(thd)_3$ and 1–10 s for pyridinedicarboxylic acid. For the further experiments we then fixed precursor/purge pulse lengths as follows: 1-s $Eu(thd)_3$/2-s N_2/2-s pyridinedicarboxylic acid/4-s N_2. It was also confirmed

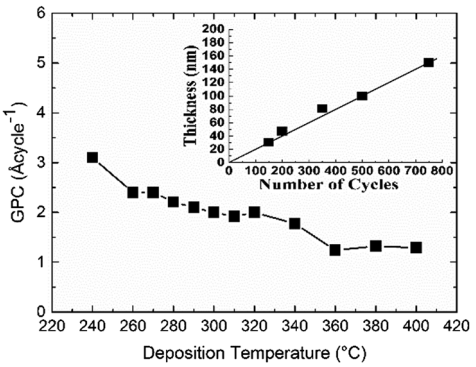

Fig. 2 Growth per cycle (GPC) at different deposition temperatures for the present Eu-hybrid thin films; the inset shows the total film thickness as a function of number of deposition cycles for films deposited at 300 °C. Experimental error bars are estimated to be within the datum point square marks.

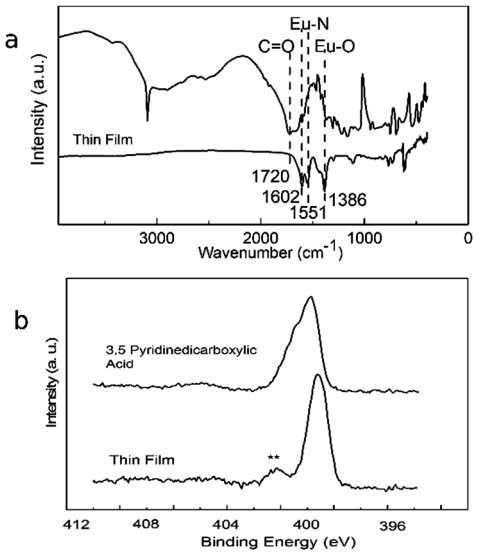

Fig. 3 (a) FTIR spectra, and (b) N-XPS spectra for 3,5-pyridine dicarboxylic acid (top) and a 100 nm thick Eu-hybrid thin film deposited at 290 °C (bottom).

that the films nucleated and grew in a similar manner on various substrate materials such as silicon, quartz, borosilicate glass, PET-ITO, polyamides and others; note that *e.g.* PET-ITO was selected because it is a commonly used flexible substrate in many applications and also readily commercially available. In Fig. 2 we plot the growth-per-cycle (GPC) values at different deposition temperatures calculated from the resultant film thickness values determined by XRR measurements. It is seen that as is typical for the inorganic–organic hybrid materials grown by ALD/MLD the thickness decreases with increasing deposition temperature.[22] For the film quality an optimum deposition temperature range was estimated to be between 260 and 340 °C, but homogeneous films were found to be formed even at temperatures down to 200 °C or up to 400 °C. In the inset of Fig. 2 we demonstrate the essentially ideal ALD/MLD behaviour, *i.e.* linear dependency of the film thickness on the number of ALD/MLD cycles, for films deposited at 300 °C.

Our Eu-hybrid films were amorphous from XRD measurement (not shown here). They were confirmed to be essentially pure from XPS data, with the following approximate elemental compositions: 62% C, 25% O, 6% N, 7% Eu, which are in reasonable agreement with the suggested film structure (Fig. 1). The films were shiny in appearance, and could be handled and stored in ambient air for a year without side reactions. From heat-treatment experiments carried out in an N_2 gas flow it was confirmed that the films remained stable at temperatures at least up to 500 °C.

In Fig. 3(a) we display FTIR spectra for a representative Eu-hybrid thin-film sample and for a free 3,5-pyridine di-carboxylate ligand for comparison; the spectrum for the Eu-hybrid film is perfectly consistent with the schematic structure of the films presented in Fig. 1. The ν(C═O) (–COOH) stretching frequency of the free 3,5-pyridinedicarboxylate ligand at 1700 cm^{-1} is absent in the spectrum of the Eu-hybrid film. The characteristic peak for ν(C═O) is observed at 1396 cm^{-1}. This frequency implies that the oxygen atoms of the carboxylate groups are coordinated to the Eu^{3+} ion. The stretching vibrations of the C═N bond in the pyridine ring are shifted to 1602 cm^{-1} and 1551 cm^{-1} for the Eu-hybrid film indicating that pyridine participates in the coordination to europium.[24–28] The absence of the broad absorption band at 3200–3500 cm^{-1} confirms that the Eu-hybrid film is devoid of OH and NH bonds, as expected. The XPS high-resolution regional spectrum of N 1s signal (Fig. 3(b)) for the same Eu-hybrid film sample is in line with our conclusions based on the FTIR data, that is, the spectrum shows a small but clear extra component (marked by asterisk in Fig. 3(b)) of a distinct chemical state for the Eu-hybrid in comparison to the spectrum for the free 3,5-pyridinedicarboxylate ligand, which could be attributed to the suggested N–Eu═O bond, although this is only one possible interpretation.

In Fig. 4 we display the UV-Visible spectrum for our Eu-hybrid thin-film sample grown on a quartz substrate. The broad and asymmetric absorption band around 270 nm (37 100 cm^{-1}) is assigned to the combination of n–π* and π–π* transitions of pyridine molecules (HOMO–LUMO) transitions:[29–31] the highest occupied ground state orbital (HOMO) and the second highest

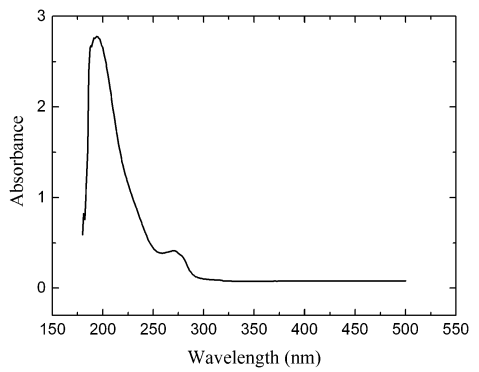

Fig. 4 UV-Vis spectrum for a 100 nm thick Eu-hybrid thin film deposited at 290 °C on a quartz substrate.

occupied orbital (SHOMO) in pyridine molecules correspond to nonbonding (or poorly binding) p orbitals of pyridine plane, and the lowest unoccupied orbitals (LUMO) correspond to the π-antibonding orbitals in the pyridine ring. An excited electron at a higher energy orbital (in LUMO) is more easily donated than a ground state electron (in HOMO).[6] Electron transfer can occur either from the excited singlet or a triplet state of the donor. Following energy absorption by the ligands, intersystem crossing to a triplet state occurs and it is followed by the energy transfer to the metal. The excited ion subsequently emits the characteristic sharp bands from the f–f transitions. This pathway is generally accepted and applicable in most conditions despite of the existence of singlet energy-transfer pathway observed in some unique systems for which the triplet state lies below the emitting state.[32]

In Fig. 5 we display the photoluminescence excitation (λ_{em} = 615 nm) and emission (λ_{ex} = 270 nm) spectra for a 100 nm thick Eu-hybrid thin film deposited at 290 °C. The appearance of the intense excitation peak around 270 nm indicates the efficient repopulation of the excited states of the Eu^{3+} ions by the electrons transferred from the pyridinedicarboxylic acid molecules. The photoluminescence emission spectrum exhibits the characteristic intense narrow bands from the $^5D_0$–^7F_J transitions (where J = 0–4)[6] of trivalent europium resulting in red light emission upon UV excitation. Most importantly, in the inset of Fig. 5 we show a photo taken under UV illumination from a Eu-hybrid film deposited on a flexible ITO-coated PET substrate; we can observe appreciably high europium emission intensity owing to the efficient energy transfer from the organic ligands. We also like to emphasize that measured the spectrum several times for the same sample after certain time periods to confirm that no visible differences occurred in the luminescence intensity with time.

The PET-ITO substrate undergoes shrinkages at temperatures above 100 °C,[33] and therefore the stress analysis was performed for thin-film coatings deposited on a new flexible polyimide DuPont Kapton that has tolerance for high temperatures as well as good light transmittance and flexibility;[34] the coatings investigated were a 100 nm thick Eu-hybrid film and a purely inorganic ALD-grown 85 nm thick europium oxide film for reference. The depositions on polyimide substrates resulted in homogeneous films even at temperatures as high as 290 °C. No cracks were visible in our Eu-hybrid thin-film coating (Fig. 6a–c)

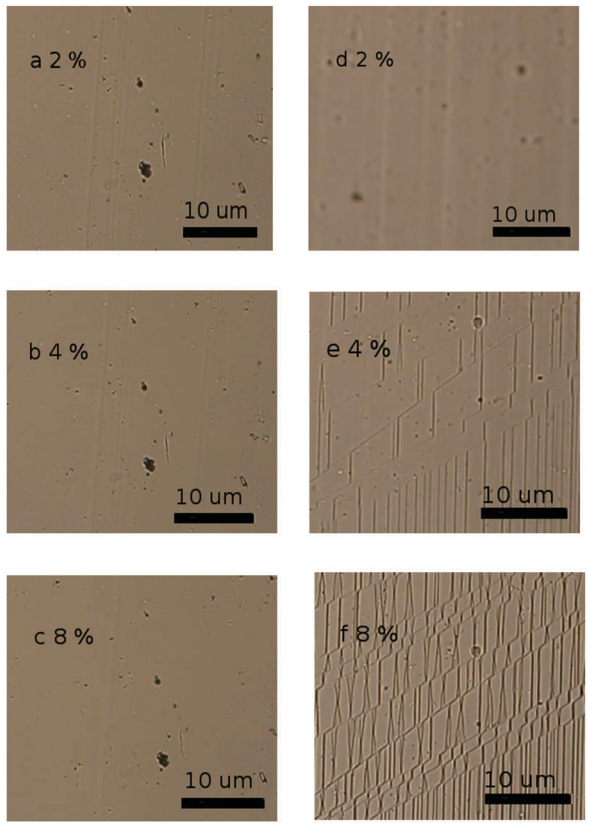

Fig. 6 Optical microscope images for a 100 nm thick ALD/MLD Eu-hybrid thin-film coating deposited at 290 °C on a polyimide substrate after the following tensile elongations: (a) 2%; (b) 4%, and (c) 8%; and for a 85 nm thick ALD Eu_2O_3 coating after the following elongations: (d) 2%; (e) 4%, and (f) 8%.

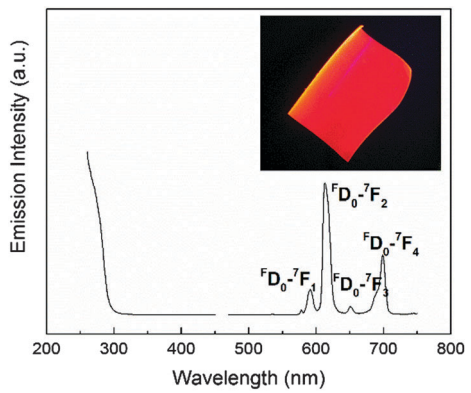

Fig. 5 Photoluminescence excitation (λ_{em} = 615 nm) and emission (λ_{ex} = 270 nm) spectra for a 100 nm thick Eu-hybrid thin film deposited at 290 °C on a quartz glass substrate; the inset shows a photo taken under 270 nm UV illumination of a similarly deposited film on an ITO-coated PET substrate.

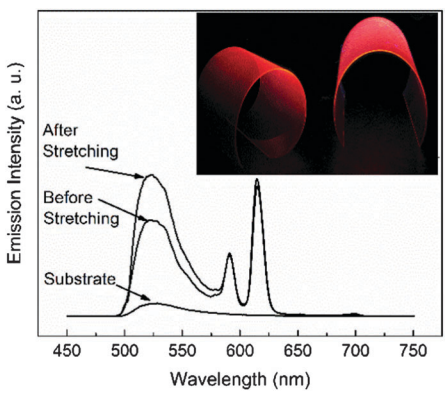

Fig. 7 Photoluminescence emission (λ_{ex} = 270 nm) spectra for a 100 nm thick Eu-hybrid thin film deposited at 290 °C on a polyimide substrate before and after stretching; the inset shows a photo taken of this Eu-hybrid coating on a transparent polyimide substrate under 270 nm UV illumination.

up to the maximum elongation point (44%), neither there were observed any effects on its photoluminescence properties. In contrast to the case of the Eu-hybrid films, on the surface of the europium oxide reference film there was observed cracking propagation within increasing tensile elongation (Fig. 6d–f).

No defects were observed for our Eu-hybrid thin films after they had been repeatedly stretched 30 times up to 3% tensile elongation and bended 600 times according to the reference.[35] Similarly, no differences in the red europium photoluminescence intensity were observed before and after stretching or bending (Fig. 7). Hence we could conclude that our luminescent Eu-hybrid films indeed are mechanically highly flexible, as expected.[36,37]

4. Conclusions

We have demonstrated that the currently emerging ALD/MLD gas-phase thin-film technique can be used for direct deposition of new type of europium–organic hybrid materials where the organic constituent efficiently sensitizes the luminescence of europium. Our proof-of-the-concept data are for a process where $Eu(thd)_3$ and 3,5-pyridinedicarboxylic acid are employed as precursors, but we expect that there will be a number of other organic molecules which could be combined with europium for further tailoring of the structural and luminescence properties.

Our Eu-hybrid thin films were revealed to be highly uniform and amazingly stable, and most importantly to show high luminescence intensities. Moreover, preliminary mechanical testings confirmed that they are also highly flexible. Since the ALD/MLD technique – owing to the self-limiting gas-surface reactions – inherently allows the deposition of conformal coatings on a variety of substrate surfaces, we foresee that our Eu-hybrid thin films could be beneficial for many cutting-edge applications that demand ultra-thin but large-area luminescent coatings on flexible substrates.

Acknowledgements

The present work has received funding from the European Research Council under the European Union's Seventh Framework Programme (FP/2007–2013)/ERC Advanced Grant Agreement (No. 339478). DuPont company is thanked for providing with newly developed polyamide CS Series of Kapton. Thanks are also due to Dr L.-S. Johansson for carrying out the XPS measurements, Mr M. Toivonen and Ms L. Martikainen for their help in the stress analysis under optical microscope, Mr M. Ruoho and Mr T. Juntunen for their help in the bending test measurements, and Ms A. Tiihonen for her help in taking the pictures under UV light.

Notes and references

1 T. Wang, X. Yu, Z. Li, J. Wang and H. Li, *RSC Adv.*, 2015, **5**, 11570–11576.
2 X. Sang, W. Chen, P. Chen, X. Liu and J. Qiu, *J. Mater. Chem. C*, 2015, **3**, 9083–9094.
3 H. S. Quah, W. Chen, M. K. Schreyer, H. Yang, M. W. Wong, W. Ji and J. J. Vittal, *Nat. Commun.*, 2015, **6**, 7594, DOI: 10.1038/ncomms8954.
4 N. B. Lima, S. M. Gonçalves, S. A. Júnior and A. M. Simas, *Sci. Rep.*, 2013, **3**, 2395, DOI: 10.1038/srep02395.
5 S. Di Pietro, D. Imbert and M. Mazzanti, *Chem. Commun.*, 2014, **50**, 10323–10326.
6 C. Truillet, F. Lux, T. Brichart, G. W. Lu and Q. H. Gong, *J. Appl. Phys.*, 2013, **114**, 114308.
7 E. S. Andreiadis, *Luminescent lanthanide architectures for applications in optoelectronics*, PhD thesis, Joseph-Fourier University, 2009.
8 Q.-F. Li, D. Yue, W. Lu, X. Zhang, C. Li and Z. Wang, *Sci. Rep.*, 2015, **5**, 8385, DOI: 10.1038/srep08385.
9 S. Biju, Y. K. Eom, J.-C. G. Bünzli and H. K. Kim, *J. Mater. Chem. C*, 2013, **1**, 6935–6944.
10 A. Beeby, *J. Chem. Soc., Perkin Trans. 2*, 1999, 493–504.
11 H. Liu, H. Wang, T. Chu, M. Yu and Y. Yang, *J. Mater. Chem. C*, 2014, **2**, 8683–8690.
12 Y. Zhang, J. J. Magan and W. J. Blau, *Sci. Rep.*, 2014, **4**, 4822, DOI: 10.1038/srep04822.
13 T. Suntola and J. Antson, *Method for producing compound thin films*, *US Pat. Appl.*, 4058430, 1977.
14 V. Miikkulainen, M. Leskelä, M. Ritala and R. L. Puurunen, *J. Appl. Phys.*, 2013, **113**, 021301.
15 M. Knez, K. Nielsch and L. Niinistö, *Adv. Mater.*, 2007, **19**, 3425–3438.
16 T. Yoshimura, S. Tatsuura, W. Sotoyama, A. Matsuura and T. Hayano, *Appl. Phys. Lett.*, 1992, **60**, 268–270.
17 A. A. Dameron, D. Seghete, B. B. Burton, S. D. Davidson, A. S. Cavanagh, J. A. Bertrand and S. M. George, *Chem. Mater.*, 2008, **20**, 3315–3326.
18 O. Nilsen, K. B. Klepper, H. Ø. Nielsen and H. Fjellvåg, *ECS Trans.*, 2008, **16**, 3–14.
19 Q. Peng, B. Gong, R. M. VanGundy and G. N. Parsons, *Chem. Mater.*, 2009, **21**, 820–830.
20 A. Sood, P. Sundberg, J. Malm and M. Karppinen, *Appl. Surf. Sci.*, 2011, **257**, 6435–6439.
21 P. Sundberg and M. Karppinen, *Eur. J. Inorg. Chem.*, 2014, 968–974.
22 P. Sundberg and M. Karppinen, *Beilstein J. Nanotechnol.*, 2014, **5**, 1104–1136.
23 K. J. Eisentraut and R. E. Sievers, *J. Am. Chem. Soc.*, 1965, **87**, 5254–5256.
24 Q.-M. Wang and B. Yan, *J. Photochem. Photobiol., A*, 2006, **177**, 1–5.
25 R. M. Silverstein, F. X. Webster and D. J. Kiemle, *Spectroscopic Identification of Organic Compounds*, John Wiley and Sons Inc., New York, 7th edn, 2005, p. 108.
26 H.-M. Ye, N. Ren, J.-J. Zhang, S.-J. Sun and J.-F. Wang, *New J. Chem.*, 2010, **34**, 533–540.
27 K. R. Surati, *Spectrochim. Acta, Part A*, 2011, **A79**, 272–277.
28 H. Xiao, M. Chen, C. Mei, H. Yin, X. Zhang and X. Cao, *Spectrochim. Acta, Part A*, 2011, **A84**, 238–242.
29 J.-M. Senegas, G. Bernardeinelli, D. Imbert, J.-C. G. Bunzli, P.-Y. Morgantini, J. Weber and C. Piquet, *Inorg. Chem.*, 2003, **42**, 4680–4695.

30 O. L. Malta, *J. Lumin.*, 1997, **71**, 229–236.
31 W. F. Sager, N. Filipescu and F. A. Serafin, *J. Phys. Chem.*, 1965, **69**, 1092–1100.
32 J.-C. G. Bunzli and S. V. Eliseeva, *Comprehensive Inorganic Chemistry II: From Elements to Applications*, 2013, vol. 8, pp. 339–398.
33 H. Kang, S. Lung, S. Leng, G. Kim and K. Lee, *Nat. Commun.*, 2015, **6**, 6503, DOI: 10.1038/ncomms7503.
34 H.-J. Ni, J.-G. Liu, Z.-H. Wang and S.-Y. Yang, *Ind. Eng. Chem. Res.*, 2015, **28**, 16–27, DOI: 10.1016/j.jiec.2015.03.013.
35 Standard 47/2199/NP: Bending test method for conductive thin films on flexible substrates, http://www.iec.ch/dyn/www/f?p=103:30:0::::FSP_ORG_ID,FSP_LANG_ID:1251,25/home-e.htm.
36 M. Vähä-Nissi, P. Sundberg, E. Kauppi, T. Hirvikorpi, J. Sievänen, A. Sood, M. Karppinen and A. Harlin, *Thin Solid Films*, 2012, **520**, 6780–6785.
37 S.-H. Jen and S. M. George, *ACS Appl. Mater. Interfaces*, 2013, **5**, 1165–1173.